The Clear-Sky Greenhouse Effect Sensitivity to a Sea Surface Temperature Change

J. PH. DUVEL

Laboratoire de Météorologie Dynamique du C.N.R.S., Ecole Polytechnique, Palaiseau, France

F. M. BRÉON

California Space Institute, Scripps Institution of Oceanography, La Jolla, California

(Manuscript received 13 October 1990, in final form 17 April 1991)

ABSTRACT

The clear-sky greenhouse effect response to a sea surface temperature (SST or T_S) change is studied using outgoing clear-sky longwave radiation measurements from the Earth Radiation Budget Experiment (ERBE). Considering geographical distributions for July 1987, the relation between the SST, the greenhouse effect G (defined as the outgoing infrared flux trapped by atmospheric gases), and the precipitable water vapor content (W), estimated by the Special Sensor Microwave Imager (SSM-I), are analyzed first. A fairly linear relation between W and the normalized greenhouse effect g, defined as $G/\sigma T_S^4$, is found. On the contrary, the SST dependence of both W and g exhibits nonlinearities with, especially, a large increase for SST above 25°C. This enhanced sensitivity of g and W can be interpreted in part by a corresponding large increase of atmospheric water vapor content related to the transition from subtropical dry regions to equatorial moist regions.

Using two years of data (1985 and 1986), the normalized greenhouse effect sensitivity to the sea surface temperature is computed from the interannual variation of monthly mean values. Although subject to uncertainties, results show a smooth variation over the 0°–32°C temperature range. A maximal sensitivity of g ($\sim 10 \times 10^{-3}$ K^{-1}) is found for both extreme temperature ranges (0°–4° and 28°–32°C), while a minimal sensitivity ($\sim 6 \times 10^{-3}$ K^{-1}) is found in the 12°–16°C temperature range. The enhanced greenhouse effect sensitivity in the warmest temperature intervals is tentatively explained by increased convection that injects water vapor into the middle and upper atmosphere. In the coldest temperature ranges, the atmosphere is dry and implies more nonsaturated absorption bands and, therefore, higher sensitivity to water vapor content. These values are related to a small interannual variation of outgoing longwave flux with SST (~ 1 W m^{-2} K^{-1}), while without water vapor feedback, this sensitivity would be on the order of 4 W m^{-2} K^{-1}.

1. Introduction

Water vapor is the atmospheric constituent responsible for the strongest absorption and absorption variability in the longwave (4–100 micron) spectral domain. Water vapor is, therefore, the gas most responsible for the so-called greenhouse effect and has a large potential response to an initial change of external forcing (incoming solar flux, anthropogenic increase of concentrations of gases such as CO_2, CH_4, or CFCs). Water vapor feedback is a major source of uncertainty in regard to climate change. Note that water vapor concentration variations affect not only longwave atmospheric absorption but also solar radiation absorption and, indirectly, the cloud radiative forcing. These feedbacks on climate, as well as others, can be important. The present study focuses, however, on the greenhouse water vapor feedback in clear-sky conditions.

A recent study by Raval and Ramanathan (1989, hereafter referred to as RR) presents an interesting method for an observational determination of the greenhouse effect over the oceans and its variation with sea surface temperature. This method uses satellite measurements of the clear-sky outgoing longwave radiation from ERBE (Earth Radiation Budget Experiment) and the sea surface temperature (SST). The greenhouse effect G is defined as the difference in upwelling longwave radiation between the surface and the top of the atmosphere. A "normalized" greenhouse effect g is defined as the ratio of G and the surface emission σT_S^4. Raval and Ramanathan shows a close to linear increase of g with the SST, which is attributed to atmospheric water vapor content variations. The RR statement is that the atmospheric water vapor content is mainly driven by the SST through the Clausius–Clapeyron relation (which relates the temperature and saturation water vapor pressure). Moreover, the g–SST mean slope shows a dramatic increase for SST greater than 25°C, which is explained either by a nonlinear dependence of the H_2O continuum opacity or by a latitudinal dependence of both precipitable water and

Corresponding author address: Jean Philippe Duvel, Centre National de la Recherche Scientifique, Laboratoire de Météorologie Dynamique du CNRS, Ecole Polytechnique, 91128 Palaiseau Cedex, France.

SST. From these results, we may expect to deduce the greenhouse effect sensitivity to the SST and, then, to obtain an estimate of the clear-sky water vapor feedback.

However, as noted in RR, atmospheric water vapor content is not only a function of the local SST, it also depends on vertical mixing as well as the large-scale circulation by way of convergence and divergence of water vapor fluxes, mainly at lower levels. The resulting *geographical* dependence of SST and water vapor, which leads to the RR relation, may then not reflect a *temporal* dependence. A better way to estimate the greenhouse effect sensitivity to the surface temperature is rather the use of interannual variability of both parameters. It is worth noting that, owing to the very different time scales of the SST and the atmospheric water vapor cycle, the mean SST–g dependence observed in interannual variation describes the atmospheric response to SST change and not the opposite.

In this paper we describe and discuss the interannual clear-sky greenhouse effect sensitivity to a sea surface temperature change. Results are used to understand the higher greenhouse effect increase with SST, as found for temperatures greater than 25°C. Data and methods are described in section 2. In section 3, we study the monthly mean relation (i.e., geographical) between the greenhouse effect, the SST, and the atmospheric water vapor content. Results on the interannual sensitivity are presented in section 4 and discussed in section 5. A summary and a conclusion are given in section 6.

2. Data and method

Three satellite-derived climatic parameters are used for our study. These are top-of-the-atmosphere clear-sky longwave flux, atmospheric water vapor content, and sea surface temperature.

The Earth Radiation Budget Experiment (ERBE) makes use of three satellite-based identical scanners to determine top-of-the-atmosphere (TOA) longwave and shortwave radiation fluxes. An important improvement in regard to previous similar experiments is that clear and cloudy scenes can be distinguished in order to compute clear-sky fluxes at the top-of-the-atmosphere and the cloud radiative forcing. We used the clear-sky flux ($M_{\mathrm{LW_{CS}}}$), as determined by the ERBE algorithm (Wielicki and Green 1989). The accuracy for regional monthly mean values is estimated to be ±5 W m^{-2}. At the time of this study, the two first years (1985 and 1986) of ERBE observations (using measurements from *NOAA-9* and ERBS satellites) have been processed in addition to July 1987 observations from ERBS and *NOAA-10* satellites. The interannual variations were, therefore, obtained on the basis of the two years 1985 and 1986. Only one satellite ERBE product has been used for January 1985 and November 1986 (ERBS).

Water vapor amount in the atmosphere was derived from the Special Sensor Microwave Imager (SSM-I) on board a Defense Meteorological Satellite Program (DMSP) satellite using an algorithm developed by Wentz (1984). Passive microwave radiometry makes it possible to infer total atmospheric water vapor content in oceanic regions where no highly precipitating clouds are present. A study, now in progress at the California Space Institute, on globally distributed in situ observations and satellite estimates shows an rms difference of the order of 10%–15% and almost no bias. Monthly values used in this study are expected to be of even better accuracy, assuming that the instantaneous errors are at least partially uncorrelated. Note that SSM-I was launched in mid-1987, and therefore, only July 1987 can be compared to ERBE observations.

Sea surface temperatures used in our study are monthly mean results of blended satellite and in situ observations processed using a method developed by Reynolds (1988). The mean accuracy of this dataset was found to be better than 1°C when compared to drifting buoys.

As was done in RR, we define the greenhouse effect as

$$G = \sigma T_S^4 - M_{\mathrm{LW_{CS}}}\ (\mathrm{W\ m^{-2}}), \tag{1}$$

where T_S is the SST. The "normalized" greenhouse effect, defined in order to remove the large surface emission dependence, is

$$g = \frac{\sigma T_S^4 - M_{\mathrm{LW_{CS}}}}{\sigma T_S^4}. \tag{2}$$

The dimensionless parameter g is, therefore, analogous to a "longwave flux absorptance" and would strictly be so if there was no emission by the atmosphere. As stated in RR, g variations are mainly driven by atmospheric water vapor. At wavelengths for which the atmosphere is opaque, the outgoing longwave radiation is insensitive to temperature and water vapor changes in the lower troposphere. It is likely that water vapor pressure is influenced by the local SST mostly in the lower atmospheric layers. The variations of g that are correlated with the local SST should, therefore, be mainly driven by atmospheric absorption variation in the atmospheric window (H_2O continuum) and in weak water vapor absorption bands.

Values of G, T_S, and g over the oceans were processed on the ERBE S9 (2.5° resolution) grid (Barkstrom et al. 1989). The local interannual sensitivity of g to a SST change is computed on the basis of $\Delta g = g_{86} - g_{85}$ and $\Delta T_S = T_{S_{86}} - T_{S_{85}}$, where g_{86}, g_{85}, $T_{S_{86}}$, and $T_{S_{85}}$ are 2.5° × 2.5° monthly mean regional values. These month-by-month interannual variations are usually small and within the data uncertainties. Moreover, we are seeking the correlated interannual changes of g and the SST, but local uncorrelated variations might be as large, if not larger. These two noise sources, data uncertainties and uncorrelated variations, are responsible for a large scatter around the mean (Δg, ΔT_S)

slope. The mean greenhouse effect sensitivity to the SST is obtained through a linear regression in the (Δg, ΔT_S) observation set. In order to limit the uncertainties, the regions for which the interannual SST change is smaller than 1°C are not considered.

3. Geographical dependence of SST, precipitable water, and the greenhouse effect

a. Relation between SST and precipitable water

To gain a better understanding of the interrelation of the different parameters, we first study their geographical distributions. Raval and Ramanathan showed that the observed increase of g with the SST is mainly driven by a coincident precipitable water (W) increase. We, therefore, first compare the SST and W geographical distributions. Their interdependence has been studied in RR and Stephens (1990), but, to our knowledge, this is the first time such a study has been done using SSM-I observations. Results are presented in Fig. 1 for July 1987 showing the mean water vapor amount for each 2°C SST interval between 2° and 30°C, which is the averaged water vapor content of all 2.5° × 2.5° regions having an SST within the 2°C range. Also reported in Fig. 1 is the standard deviation of W for each SST interval (error bars) as well as the result of a semiempirical relation. This last was obtained combining the Clausius–Clapeyron relation, which yields water vapor saturation pressure as a function of temperature, and Smith's (1966) empirical formula, which gives the atmospheric water vapor content as a function of surface water vapor pressure. The resulting equation is (Stephens 1990):

$$W = 108.2 \frac{r}{1+\lambda} e^{0.064(T_s-288)} \text{ (kg m}^{-2}\text{)} \quad (3)$$

where r is the relative humidity at the surface and λ the ratio between the atmospheric pressure scale height and the water vapor pressure scale height. Although the ratio $r/(1+\lambda)$ is variable with latitude and season, we show the water vapor content as a function of T_S for $r/(1+\lambda) = 0.2$, a typical value. Note that this ratio increases with the surface relative humidity and with the water vapor scale height.

The mean relation between the observed water vapor (W) and the SST appears nonlinear. The water vapor content increase observed from cold to warm areas can be explained by the growth, in the lower layer, of the atmospheric water vapor capacity related to the sea surface temperature through the Clausius–Clapeyron relation. However, the atmospheric water vapor content is also strongly modified by water vapor horizontal divergence and vertical mixing, leading to variations of the ratio $r/(1+\lambda)$ from one region to another. As expected, because of these variations of $r/(1+\lambda)$, the linear fit into the values is then not parallel to the slopes given by Eq. (3).

It is not straightforward to analyze the slope of the mean SST–g geographical relation. We give a tentative explanation using a rough division of the graph in three parts and assuming that the SST distribution is mostly latitudinal. For SST greater than 20°C, the mean slope is larger than the Clausius–Clapeyron slope, which may be interpreted as an enhanced increase in water vapor content from subtropical (dry) low-level divergence regions to equatorial (moist) low-level convergence regions (ITCZ). It is worth noting that this part extends latitudinally roughly from 30°S to 40°N and represents more than half of oceanic regions. The second part, roughly between 10°C and 20°C, has a slope smaller than the Clausius–Clapeyron slope, which may be interpreted as the inverse effect (i.e., the reduced increase of precipitable water from midlatitude low-level convergence regions to subtropical divergence regions). The third part (0°–10°C), while more noisy, seems to be in better agreement with the Eq. (3) slope, perhaps because the latitudinal W gradient is less perturbed by convergence variations in subpolar regions, leading to a weaker deformation of the curve from one temperature interval to another.

When considering the whole temperature range, the slope of the best fit between SST and $\ln(W)$ is found to be 0.051 K^{-1}. Considering only the high-temperature range ($T > 25$°C), the mean slope increases strongly and reaches 0.098 K^{-1}. This shows that at least part of the nonlinearity of the g–SST relation, mentioned in RR, can be attributed to a nonlinearity of the geographical W increase with SST.

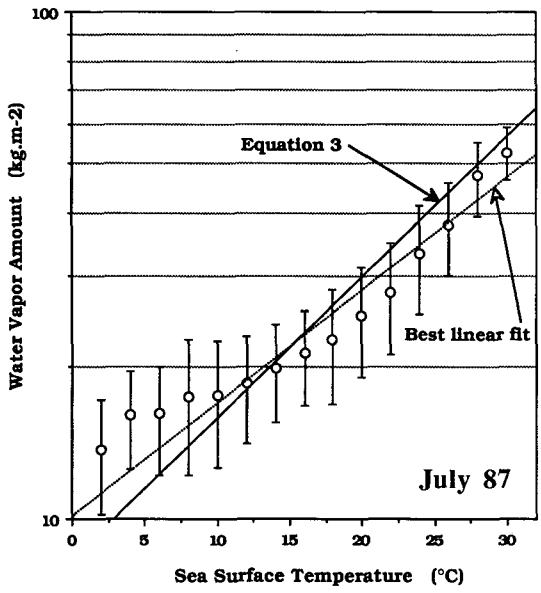

FIG. 1. Geographical dependence between the SST and the precipitable water W on the basis of July 1987 regional mean values. The error bars represent the standard deviation of W within a given SST interval. Also reported are the best linear fit between $\ln(W)$ and the SST, computed on the basis of all W–SST couples, and the slope given by Eq. (3) with $r/(1+\lambda) = 0.2$.

b. Relation between g and the precipitable water

July 1987 is the one month for which concomitant ERBE and SSM-I products are available. We therefore study the mean relation between W and g on monthly 2.5° × 2.5° averages. Figure 2 shows the monthly mean relation between the atmospheric water vapor content and the normalized greenhouse effect. The mean value is shown with the standard deviation for each 2 kg m^{-2} intervals of water vapor. For $W \geq 15$ kg m^{-2}, mean values of g are distributed almost perfectly on a straight line, with a best fit equal to

$$g = 0.045 + 8.68 \times 10^{-2} \ln(W). \quad (4)$$

For water vapor amount smaller than 15 kg m^{-2}, mean values of g show an asymptotic behavior. Since few points are involved, the observed tendency may not be statistically significant, and further studies are needed to confirm it.

A temperature of 25°C corresponds, on average, to an atmospheric water vapor content of 35 kg m^{-2} (Fig. 1). We therefore looked for a possible nonlinear dependence of the water vapor opacity by computing the mean slope between $\ln(W)$ and g for water vapor amounts lower and higher than this threshold. Although the precipitable water is strongly coupled with the SST, no significant difference was found, suggesting that the steep increase of the normalized greenhouse effect for high SSTs should not be attributed to the W–g dependence. This does not exclude, however, a dependence between g and SST for a given W, which could not be taken into account by the simple σT_S^4 normalization (impact of the nonlinearity of the H_2O continuum absorption).

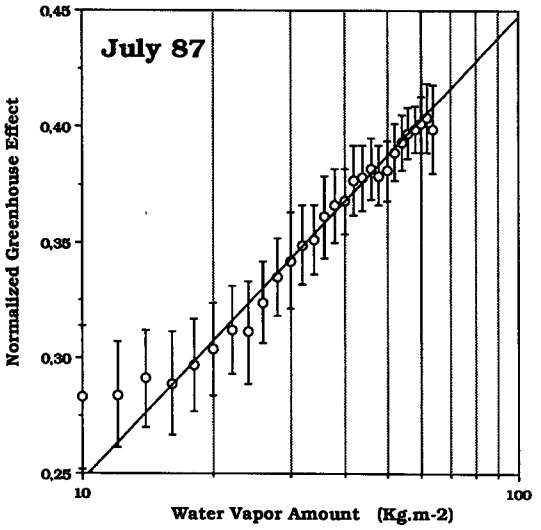

FIG. 2. Normalized greenhouse effect g as a function of the precipitable water W on the basis of July 1987 regional mean values. Error bars represent the standard deviation of g in a given W interval. Also shown is the best linear fit of g as a function of $\ln(W)$.

Because no reliable global water vapor observations were available to RR during the same period as ERBE, they chose to study the water vapor–g dependence using measurements of April 1982 (water vapor from SMMR) and April 1985 (greenhouse effect). Moreover, in order to limit the uncertainties, they used zonal averages; that is, all oceanic values within each 2.5° latitude band were averaged to derive one point. They reported:

$$g_{85} = 0.155 + 5.76\ 10^{-2} \ln(W_{82}),$$

which is different from that given by Eq. (4). Note that the difference for the intercept is only a secondary effect resulting from the different slopes. The slope difference had to be investigated. It could be the consequence of the use of zonal averages instead of box averages, the use of different seasons, a bias between SSMR water vapor retrievals and SSM-Is, or the fact that RR compares nonconcomitant observations (W of April 1982 and g of April 1985).

1) Using our own July 1987 dataset, we investigated the consequence of zonal averaging. The best fit through zonal averaged values is

$$g = 0.0458 + 8.71\ 10^{-2} \ln(W) \quad (R^2 = 0.94),$$

which is very close to the fit obtained with box averages. The first hypothesis can therefore be rejected.

2) The use of different seasons (July instead of April) cannot be ruled out a priori as a source of the discrepancy. However, our study was done globally and, therefore, included two opposite seasons. No significant difference was found between Northern and Southern hemispheres, suggesting that the relation does not strongly depend on either season or hemisphere.

3) SMMR and SSM-I are similar instruments and both showed the quality of their water vapor retrievals (Alishouse 1983; Alishouse et al. 1990). Note that the slope difference concerns the logarithm of the water vapor and, therefore, the water vapor bias between the two instruments would have to be very large to explain the differences. This hypothesis can therefore be ruled out.

4) The uncertainty inherent in the use of nonconcomitant observations could be tested with our own dataset by comparing zonal averages of the water vapor retrieval of July 1987 and of the greenhouse effect of July 1985. The correlation was lower ($R^2 = 0.88$) but still large enough to obtain a meaningful slope. The best fit is

$$g_{85} = 0.112 + 6.82\ 10^{-2} \ln(W_{87}),$$

which gives a third rather different slope. It shows that interannual variations of g and/or W can be large enough to induce changes to the best-fit slope of at least 30%. It is therefore essential to use simultaneous observations to find a meaningful relation between g and W.

c. *Relation between g and the SST*

The mean relation between the regional monthly means of the normalized greenhouse effect g and the SST for 1985 and 1986 (Fig. 3) resembles what was found for the relation between $\ln(W)$ and the SST for July 1987 (Fig. 1). This agreement was predictable since there is a fairly linear relation between g and $\ln(W)$. It confirms that the geographical relation between the greenhouse effect and the SST is primarily driven by the water vapor amount and is then also very dependent on the geographical distributions of both SST and W.

Because the geographical dependence of the sea surface temperature and the greenhouse effect may not reflect their mutual temporal variation, this dependence should not be used to forecast the greenhouse effect change subsequent to a climatic SST change.

4. Greenhouse effect sensitivity to interannual SST changes

Figure 4 shows the sensitivity of g to the SST for different temperature intervals on the basis of month by month interannual variations between 1985 and 1986. These sensitivities, S, are the slopes obtained by a linear fit through the regional values of $\Delta g = g_{86} - g_{85}$ as a function of $\Delta T_S = T_{S_{86}} - T_{S_{85}}$, where g_{86}, g_{85}, $T_{S_{86}}$, and $T_{S_{85}}$ are 2.5° × 2.5° monthly mean regional values. Here S is given as the least-squares fit to $\Delta g = S\,\Delta T_S$, i.e.,

$$S = \frac{\sum_{i=1}^{N} \Delta_i g \Delta_i T_S}{\sum_{i=1}^{N} (\Delta_i T_S)^2}, \qquad (5)$$

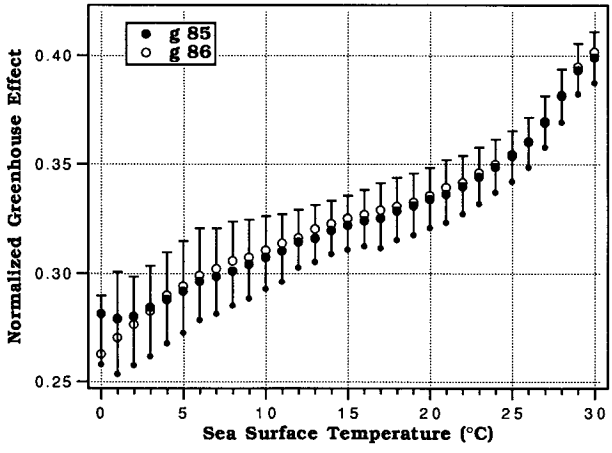

FIG. 3. Normalized greenhouse effect g as a function of the SST on the basis of 2.5° × 2.5° monthly mean regional values for 1985 and 1986. Error bars (upward for 86 and downward for 85) represent the standard deviation of g in a given SST interval.

where the sums are made over the ERBE regions for which the SST is within the chosen range (4°C SST intervals from 0°C) and for which $|\Delta T_S| > 1$°C. The error bar extensions E give an indication of the scatter around the best slope for each temperature interval:

$$E^2 = \frac{\sum_{i=1}^{N} (\Delta_i g - S\Delta_i T_S)^2}{\sum_{i=1}^{N} (\Delta_i T_S)^2}. \qquad (6)$$

Note that the statistical uncertainty on the mean sensitivity is given by $E/\sqrt{N-2}$, where N is the number of observations (considered as independent) also reported in Fig. 4. Despite the relatively large value of E for each temperature interval, and then of the measurement scatter around the best linear fit, we find a relatively stable value of the mean slopes between 6×10^{-3} and 10×10^{-3} K^{-1}. This is nearly twice the sensitivity obtained considering, as in RR, the mean slope in the regionally dependent values of g and the SST. The sensitivity varies smoothly from the lowest to the highest temperature range. A maximal sensitivity, on the order of 10×10^{-3} K^{-1}, is found for both extreme temperature ranges (0°–4° and 28°–32°C). A minimal sensitivity of 6×10^{-3} K^{-1} is measured in the 12°–16°C temperature range.

An important question is the accuracy of this result. From Eq. (2), we obtain:

$$\frac{dg}{dT_s} = 4\frac{M_{\mathrm{LW_{CS}}}}{\sigma T_S{}^5} - \frac{1}{\sigma T_S{}^4}\frac{d}{dT_S}(M_{\mathrm{LW_{CS}}}). \qquad (7)$$

If we assume that the error in $M_{\mathrm{LW_{CS}}}$ is smaller than 5 W m^{-2} and that T_S is known to better than 1°C, we find better than 3×10^{-4} accuracy for the first term on the right of Eq. (7), which varies roughly between 0.01 K^{-1} and 0.0085 K^{-1} for SST between 5°C and 25°C. Accuracy of the second term is more difficult to estimate since it makes use of an interannual variation whose accuracy is unknown. Our analysis makes implicit use of the ratio $\Delta(M_{\mathrm{LW_{CS}}})/\Delta(T_S)$ for the second term estimate, where both components of the ratio are observed interannual variations.

Using the ERBE accuracy estimate of 5 W m^{-2} for $M_{\mathrm{LW_{CS}}}$ and assuming that the measurement errors for 1985 and 1986 are uncorrelated, a standard error of 7 W m^{-2} for $\Delta(M_{\mathrm{LW_{CS}}})$ is obtained: a very large value considering that $\Delta(M_{\mathrm{LW_{CS}}})$ is on the order of 1 W m^{-2} for a 1°C SST change. However, because the interannual variation involves the monitoring of similar scenes, we may expect the measurement errors of 1985 and 1986 to be correlated, reducing the standard error of $\Delta(M_{\mathrm{LW_{CS}}})$. Moreover, the use of many different observations, as was done in this study, allows the systematic effect to be extracted from the noise. These assumptions are confirmed by the rather uniform values found over a wide range of SST. Despite a large dispersion of interannual variation of both $M_{\mathrm{LW_{CS}}}$ and

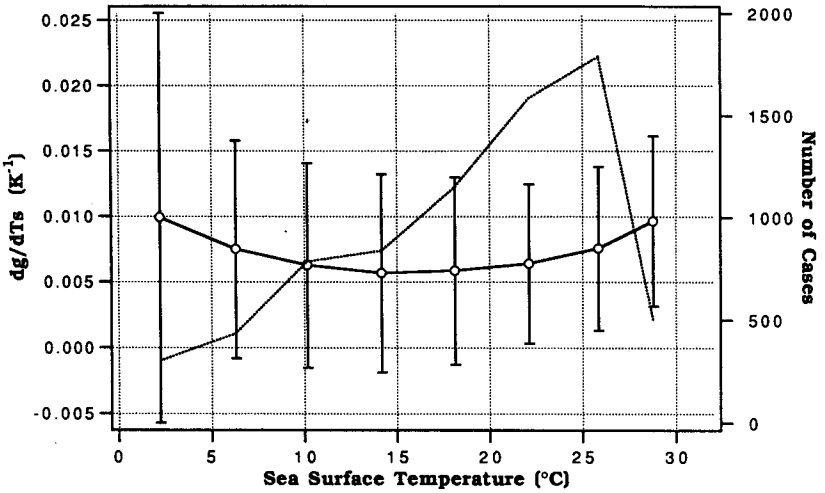

FIG. 4. Sensitivity of the normalized greenhouse effect g to an interannual change of the SST. Mean sensitivities as well as the scatter around these means, computed as described in the text, are given for 4-K SST intervals. Also reported is the number of observations in each SST interval.

the SST, a systematic trend appears in the second term of Eq. (7) and reduces dg/dT_s to a relatively stable value.

Another uncertainty on the estimate of the clear-sky outgoing longwave radiation is the cloud detection. Since the cloud detection algorithm used for ERBE observation processing makes use of infrared thresholds, there may be a biased clear-sky estimate when monitoring two scenes with different surface temperatures: i.e., a tendency to keep the longwave clear-sky flux larger than the threshold value. To investigate if there is such a cloud detection bias, we computed the clear-sky albedo interannual variations. There was no correlation with the surface temperature interannual variation, suggesting that ERBE cloud detection algorithm is not sensitive to small surface temperature variations. In addition, the number of clear-sky scenes detected also appear to be uncorrelated with the interannual variation of SST.

Assuming that the greenhouse effect sensitivity, obtained from interannual variation and presented in Fig. 4, is accurate, we now attempt to justify the curve variations, i.e., the maximal sensitivity for both extreme temperature ranges. The warmest temperature interval corresponds to deep convection zones, that is, areas of the globe where the vertical mixing involves the whole atmosphere. The positive correlation between the SST and deep convection has long been known. A recent study (Rind et al. 1991) shows that deep convection has a tendency to moisten the upper and middle atmosphere. Molecule for molecule, water vapor is more greenhouse efficient in these layers than in the lower atmospheric layers where most water vapor absorption bands are saturated. We therefore suggest that the enhanced greenhouse effect sensitivity in the warmest temperature interval results from increased convection that injects water vapor into the middle and upper atmosphere. Let us point out, however, that this process explains an enhanced sensitivity in the highest temperature interval but not the monotone increase from 15°C.

In the coldest temperature range, one can impute the enhanced sensitivity to the low atmospheric water vapor content: a dry atmosphere implies more nonsaturated absorption bands and, therefore, higher sensitivity to increased water vapor. Accounting for the saturation of absorption bands qualitatively explains the decreasing sensitivity from 0° to 15°C.

5. Implications for global climate change

Although our study concentrates on a normalized greenhouse effect, the climate implications will be based on the nonnormalized term, G, since it regulates the earth radiation balance. Extending our results obtained on the basis of interannual variation to the case of a global climate change, we project that the G–SST curve should be shifted and reshaped following

$$\frac{dG}{dT_S} = 4\frac{G}{T_S} + \frac{dg}{dT_S}\sigma T_S^4, \tag{8}$$

where dg/dT_S is obtained from Fig. 4. The first term on the right side of Eq. (8) is the greenhouse effect sensitivity for a constant g, i.e., assuming no feedback. The second term includes the water vapor feedback. Mean values of various components of Eq. (8) are given in Table 1. Note that, although interannual variations yield dg/dT_S values about twice as large as that obtained from geographical distribution, the ratio is re-

TABLE 1. Present (1985 and 1986) mean values of the TOA clear-sky longwave radiation, the greenhouse effect G, and the normalized greenhouse effect g. Also shown are these parameters' sensitivity to the sea surface temperature based on interannual variations. The last column gives the TOA longwave radiation sensitivity to the sea surface temperature, assuming a constant normalized greenhouse effect.

T_s (°C)	M_{LWcs} (W m^{-2})	G (W m^{-2})	g	dM_{LWcs}/dT_S (W m^{-2} K^{-1})	dG/dT_S (W m^{-2} K^{-1})	dg/dT_s (10^{-3} K^{-1})	$4\sigma T_S^3(1-g)$ (W m^{-2} K^{-1})
2	237	89	0.27	0.2	4.5	9.9	3.4
6	245	101	0.29	0.9	4.0	7.5	3.5
10	253	112	0.31	1.3	3.9	6.3	3.6
14	263	123	0.32	1.5	3.9	5.7	3.7
18	272	136	0.33	1.4	4.3	5.9	3.7
22	283	148	0.34	1.1	4.8	6.4	3.8
26	289	164	0.36	0.4	5.6	7.6	3.9
29	288	184	0.39	−0.7	7.0	9.7	3.8

duced, on account of the G/T_S term, when considering the nonnormalized greenhouse effect sensitivity.

Note that, in the absence of water vapor feedback, the greenhouse effect sensitivity should vary in T_S^3. Because of the relatively strong dg/dT_S found, there is a substantial additional T_S^4 dependence, which increases the sensitivity faster near the poles and in tropical regions (Table 1). In case of a global SST change, water vapor feedback may then give an additional potential perturbation in change of the equator to pole gradient of the atmospheric radiative diabatic heating by longwave radiation, which may influence the large-scale circulation.

Another quantity of interest, particularly for global change monitoring, is the TOA clear-sky longwave flux sensitivity to a surface temperature variation. Note that the TOA longwave flux, and not the greenhouse effect, is the quantity determined by experiments such as ERBE. The study of g and G, and their variations, however, are needed to understand the atmospheric radiative processes. Considering a situation with no feedbacks, i.e., assuming a constant g, the clear-sky TOA flux sensitivity to the sea surface temperature would be equal to $4\sigma(1-g)T_S^3$. Values range between 3.4 and 3.9 W m^{-2} K^{-1} for sea surface temperatures ranging between 2° and 29°C. The observed values based on interannual variations are largest (1.5 W m^{-2} K^{-1}) for sea surface temperature around 15°C and are smallest (even negative) for extreme values of the SST range corresponding to subpolar and tropical regions (see Table 1). These yield rather small TOA longwave flux variations, even with a relatively large (2°–4°C) surface temperature increase. In case of such a global temperature increase, the clear-sky longwave measurements, such as ERBE's, may show almost no variations. Combined with SST measurements, however, the enhanced greenhouse effect and the water vapor feedback should be easily detected.

6. Summary and concluding remarks

We first examined the geographical dependences between the 2.5° × 2.5° regional monthly mean of the normalized greenhouse effect g, the precipitable water vapor content W, and the SST for July 1987. The geographical relation between g and $\ln(W)$ is fairly linear for W larger than 15 kg m^{-2}. On the contrary, the geographical relations between the SST and both $\ln(W)$ and g exhibit nonlinearities. Particularly, as found by RR, the slope of the mean geographical relation between the normalized greenhouse effect g and the SST increases dramatically for sea surface temperatures higher than 25°C. This enhanced sensitivity of g to the SST based on the geographical distribution may be explained by the similar larger water vapor increase with surface temperature above the 25°C SST threshold, as observed on monthly mean SSM-I estimates. Since the SST distribution is fairly latitudinal, the enhanced atmospheric water vapor content above 25°C may result from the transition from subtropical dry regions to equatorial moist regions and, therefore, from a large precipitable water variation in relation to a relatively small SST change. From these considerations, it is deduced that the use of geographical distributions of both SST and W may lead to a biased estimate of the water vapor greenhouse feedback.

On the basis of two years of ERBE observations, we have shown that, except for SSTs larger than 25°C, the greenhouse effect response to a sea surface temperature change is larger when derived from interannual variations than when the present geographical distributions of these quantities are considered. The normalized greenhouse effect sensitivity to the surface temperature, although subject to uncertainties, shows a smooth variation over a wide range of temperature. A maximal sensitivity of g, on the order of 10×10^{-3} K^{-1}, is found for both extreme temperature ranges (0°–4°C and 28°–32°C). A minimal sensitivity of 6×10^{-3} K^{-1} is measured in the 12°–16°C temperature range. Although there is an increased greenhouse effect sensitivity in the high temperature range, no "dramatic increase" is observed on interannual variations for SSTs larger than 25°C.

The observed clear-sky outgoing longwave flux sensitivity is on the order of 1.5 W m^{-2} K^{-1} for a SST around 15°C and smaller than 0.5 W m^{-2} K^{-1} in polar

regions and in the tropics. This result is to be compared to the 4 W m^{-2} K^{-1} sensitivity without water vapor feedback. The small sensitivity found for the clear-sky outgoing longwave flux, which results from the strong water vapor feedback, implies that a large SST variation is needed to compensate a perturbation of the greenhouse effect by other gases. It suggests that negative feedbacks must be present to limit climate sensitivity to radiation balance anomaly. Since these results were obtained only for clear-sky ocean regions, it is possible that clouds induce such a negative radiative feedback. The sensitivity over land regions also needs to be investigated.

Continued accurate determination of clear-sky radiation balance will be useful in order to verify these estimates. The survey of the clear-sky greenhouse effect and its interannual variations can also be used for the validation of climate models by inferring their clear-sky atmospheric response to an SST variation. As noted in RR, another source of great interest is the greenhouse effect survey over the next 10–20 years in order to detect a climatic trend that could appear in relation to an anthropogenic increase of gases such as CO_2 and CH_4. For this purpose, both SST retrievals and accurate radiative balance measurements are needed.

Acknowledgments. The comments from two anonymous reviewers greatly helped to improve this paper. F. M. Bréon was supported in part by NASA Grant NAGW-0981. The help and comments of R. Kandel, C. Gautier, R. Frouin, and V. Ramanathan were greatly appreciated.

REFERENCES

Alishouse, J. C., 1983: Total precipitable water and rainfall determinations from the SEASAT scanning multichannel microwave radiometer. *J. Geophys. Res.*, **88,** 1929–1935.

——, S. Snyder, J. Vongsathorn and R. Ferraro, 1990: Determination of oceanic total precipitable water from the SSM-I. *IEEE Trans. Geosci. Remote Sens.*, **28**(5), 811–816.

Barkstrom, B. R., E. Harrison, G. L. Smith, R. Green, J. Kibler, R. Cess and the ERBE Science Team, 1989: Earth Radiation Budget Experiment (ERBE) archival and April 1985 results. *Bull. Amer. Meteor. Soc.*, **70,** 1254–1262.

Oort, A. H., 1983: Global atmospheric circulation statistics, 1958–1973. NOAA Prof. Paper No. 14, Rockville, Md., 180 pp.

Raval, A., and V. Ramanathan, 1989: Observational determination of the greenhouse effect. *Nature,* **342,** 758–761.

Rind, D., E.-W. Chiou, W. Chu, J. Larsen, S. Oltmans, J. Lerner, M. P. McCormick and L. McMaster, 1991: Positive water vapour feedback in climate models confirmed by satellite data. *Nature,* **349,** 500–503.

Reynolds, R. W., 1988: A real-time global sea-surface temperature analysis. *J. Climate,* **1,** 75–86.

Smith, W. L., 1966: Note on the relationship between total precipitable water and surface dew point. *J. Appl. Meteor.*, **5,** 726–727.

Stephens, G. L., 1990: On the relationship between water vapor over the oceans and sea surface temperature. *J. Climate,* **3,** 634–645.

Wentz, F. J., 1983: A model function for ocean microwave brightness temperatures. *J. Geophys. Res.*, **88,** 1892–1908.

Wielicki, B. A., and R. N. Green, 1989: Cloud identification for ERBE radiative flux retrieval. *J. Appl. Meteor.*, **28,** 1133–1146.